

# **Supporting Information for “Regrowth-Free” Fabrication of High-current-gain AlGa<sub>N</sub>/Ga<sub>N</sub> Heterojunction Bipolar Transistor with N-p-n Configuration**

Takeru Kumabe<sup>1\*</sup>, Hirotaka Watanabe<sup>2</sup>, Yuto Ando<sup>2</sup>, Atsushi Tanaka<sup>2</sup>, Shugo Nitta<sup>2</sup>, Yoshio Honda<sup>2</sup>, and Hiroshi Amano<sup>2,3,4</sup>

<sup>1</sup>*Department of Electronics, Nagoya University, Nagoya 464-8603, Japan*

<sup>2</sup>*Institute of Materials and Systems for Sustainability, Nagoya University, Nagoya 464-8601, Japan*

<sup>3</sup>*Venture Business Laboratory, Nagoya University, Nagoya 464-8603, Japan*

<sup>4</sup>*Akasaki Research Center, Nagoya University, Nagoya 464-8601, Japan*

E-mail: kumabe@nagoya-u.jp

## A. Structural properties of the fabricated AlGaN/GaN HBT

Structural properties of the fabricated AlGaN/GaN HBT were evaluated by secondary ion mass spectroscopy (SIMS) and X-ray diffraction (XRD). Since there is a trade-off between depth-resolution and detection limit in SIMS measurements, two different priorities of measurements were employed in this study. Figure A-1 shows the depth profiling of AlN mole fraction and Mg/Si concentration around the emitter-base and base-collector junctions determined by SIMS with depth-resolution priority. The average Mg/Si concentration in the n-GaN cap, n<sup>+</sup>-AlGaN emitter, and p<sup>+</sup>-GaN base were  $6.5 \times 10^{18} \text{ cm}^{-3}$ ,  $1.8 \times 10^{19} \text{ cm}^{-3}$ , and  $8.9 \times 10^{18} \text{ cm}^{-3}$ , respectively. The AlN mole fraction in the emitter layer was about  $17 \pm 3\%$ , which is in good agreement with the value determined by XRD analyses (mentioned below). It should be noted that Mg accumulated layer around the emitter-base interface was intentionally introduced to minimize Mg incorporation into the emitter and the cap layers and fix the junction plane.

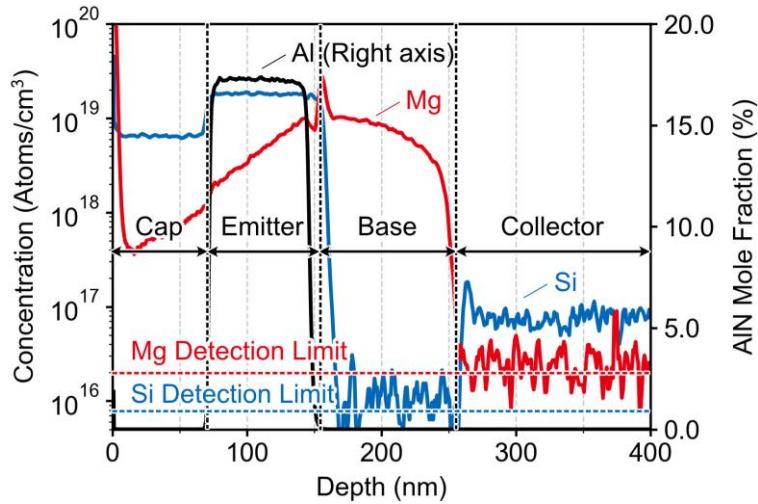


**Figure A-1:** Depth profiling of AlN mole fraction and Mg/Si concentration around the emitter-base and base-collector junctions determined by SIMS with depth-resolution priority.

Figures A-2(a) and A-2(b) show the depth profile of intentionally- and unintentionally-doped impurities, respectively. The average Si concentration in the n<sup>-</sup>-GaN collector and n-GaN subcollector were  $6.9 \times 10^{16} \text{ cm}^{-3}$  and  $1.7 \times 10^{18} \text{ cm}^{-3}$ , respectively. Although slight high Fe, C, and O were detected in the emitter and the base layer, it is hard to conclude whether it

originates from surface adsorbates or the epi-layer since they are in the very surface region. It is noteworthy that the detected Fe and C concentrations in the epi-layer were significantly low compared with intentionally-doped Si/Mg and expected free carrier concentrations and have small effects on the device characteristics even if it is really in the epi-layer. In addition, the detected Fe atoms throughout the epi-layer were arise from the Mg-source line of the MOVPE reactor and eliminated by optimizing the cleaning conditions (i.e., not due to the growth condition for the HBT structure).

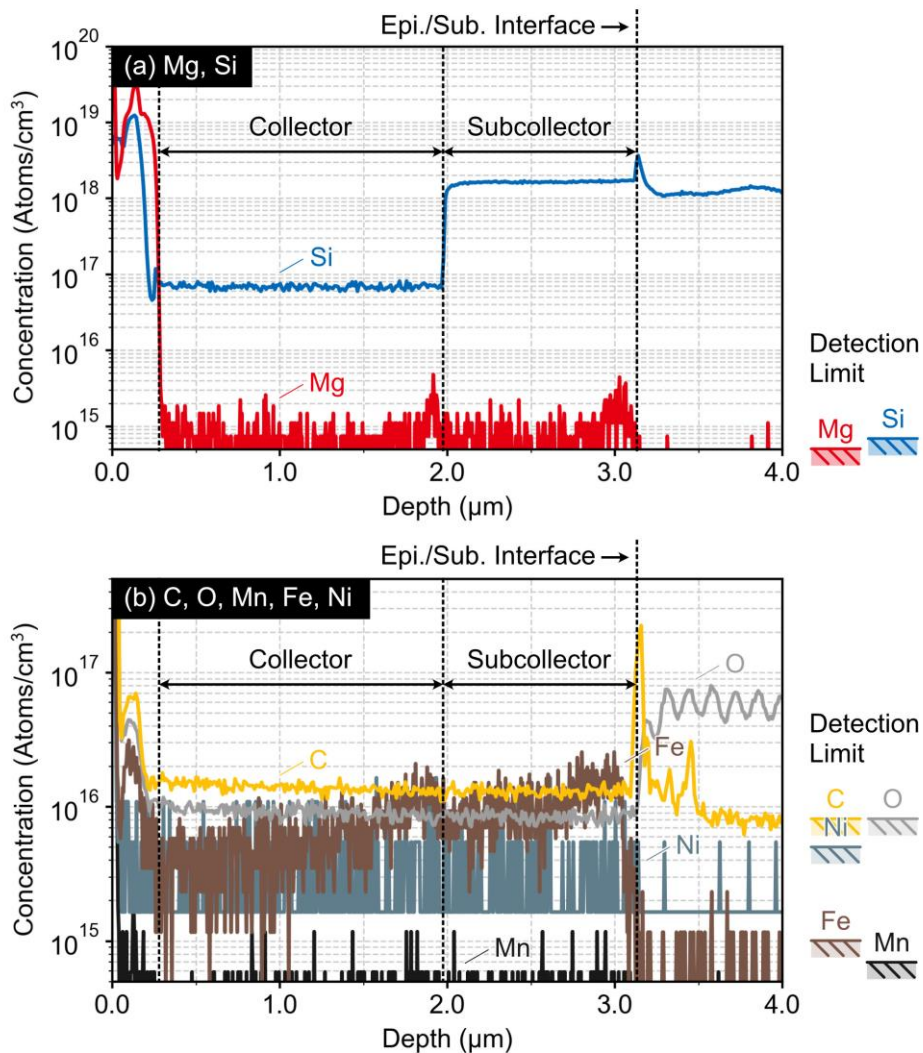


**Figure A-2:** Depth profiling of (a) intentionally-doped impurities (Mg, Si) and (b) unintentionally-doped impurities (C, O, Mn, Fe, Ni) determined by SIMS with detection limit priority.

Figures A-3(a) and A-3(b) show the XRD reciprocal space mapping (RSM) of the  $\bar{1}\bar{1}24$  plane and  $2\theta-\omega$  scan of the 0002 planes for the grown AlGaIn/GaN HBT epi-wafer, respectively. The XRD-RSM result revealed that the emitter AlGaIn layer was perfectly strained on the GaN substrate, and its AlN mole fraction was determined as 14.8% considering the lattice constants along  $a$ - and  $c$ -axes<sup>1)</sup>. Furthermore, the thickness of the n-GaN cap and the n<sup>+</sup>-AlGaIn emitter layers were calculated by fitting the result of the  $2\theta-\omega$  scan. Fig. A-3(b) shows experimental and calculated  $2\theta-\omega$  curves in the best-fitted case. The extracted thickness for the n-GaN cap and the n<sup>+</sup>-AlGaIn emitter were 65 nm and 75 nm, respectively, which are in good agreement with the values of 70 nm and 73 nm determined by SIMS. Thus, we can conclude that the AlGaIn/GaN HBT structure designed in Figure 1 is successfully realized in this study.

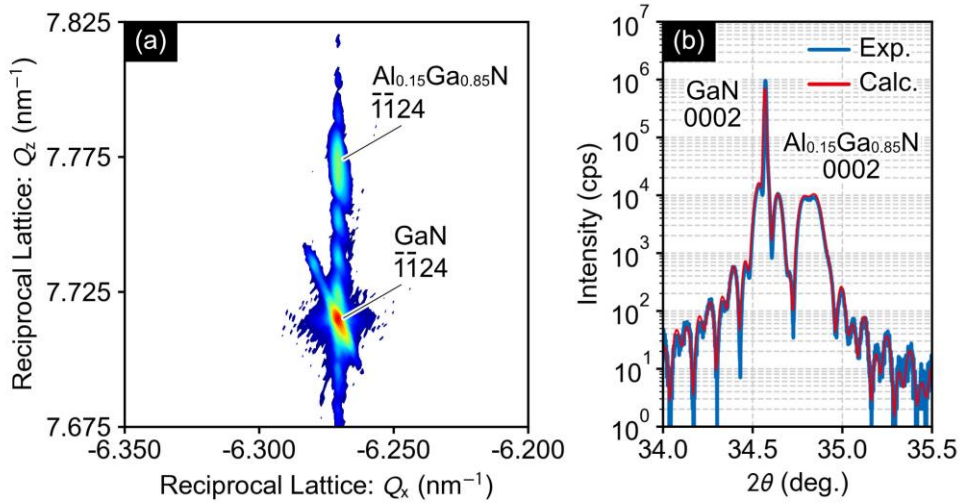


**Figure A-3:** (a) XRD-RSM of the  $\bar{1}\bar{1}24$  and (b)  $2\theta-\omega$  scan of the 0002 planes for the fabricated AlGaIn/GaN HBT epi-wafer.

## B. Energy band structure at thermal equilibrium state

Figure B-1 shows the energy band structure and carrier concentration profile in each layer for the fabricated devices at thermal equilibrium state (@300 K). Silvaco Atlas<sup>TM</sup> was employed for the calculations. The device parameters including doping levels and AlN mole fraction in the AlGaIn layer were set to the same as discussed in the previous section, and the effects of polarization charges and incomplete ionization of acceptors were also taken

into account in this calculation. Although there are large polarization charges at the AlGa<sub>N</sub>/Ga<sub>N</sub> interface, no electron or hole accumulations were observed at the emitter-base interface. Heavily doped Mg and Si around the junction contributed to eliminating the polarization charge at the interface. Therefore, performance deteriorations (e.g., low current gain) due to potential notch at the emitter-base interface induced by polarization charge should be considered in the case of devices with mildly doped emitter and base. The effective base width estimated from the band structure was about 80 nm, which is 20% smaller than that of Mg-doped Ga<sub>N</sub> thickness. Although the shrinking is inevitable as the nature of semiconductor physics, non-depleted p-GaN would be also expected in the fabricated devices (i.e., the device does not in punch-through condition unless it is not in the highly biased conditions). Thus, we can conclude that the fabricated AlGa<sub>N</sub>/Ga<sub>N</sub> HBT structure allows devices operation from the viewpoint of device physics.

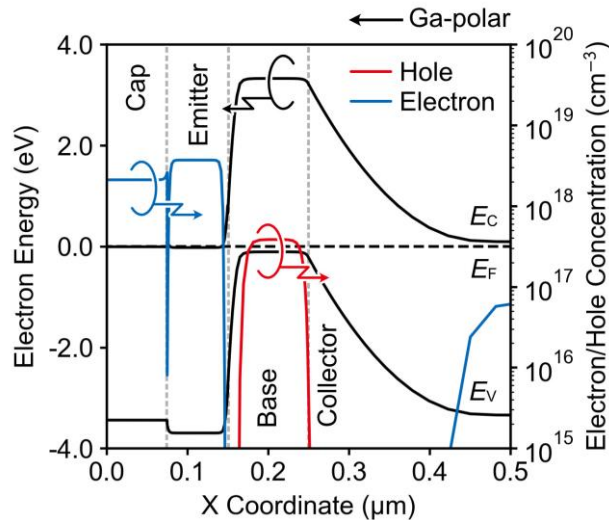


**Figure B-1:** Energy band structure and carrier concentration profile in each layer for the fabricated device at thermal equilibrium state (@300 K).

## References

- 1) O. Ambacher, B. Foutz, J. Smart, J. R. Shealy, N. G. Weimann, K. Chu, M. Murphy, A. J. Sierakowski, W. J. Schaff, L. F. Eastman, R. Dimitrov, A. Mitchell, and M. Stutzmann, J. Appl. Phys. **87**, 334 (2000).